

# Subsurface aeration evaluation

Michael B. Lakin and Ronald N. Salzman Mixing Equipment Co. Inc., Rochester, N.Y.

Subsurface aeration systems are not only receiving increased theoretical attention but are also gaining a larger share of today's aeration market. This mode of aeration is selected for a variety of reasons including land availability, operation at high power levels with minimal surface spray and mist, and the ability to achieve high uptake rates with a large degree of process flexibility. These influences combined with the magnitude of the aeration market have provided the impetus for the development of numerous types of subsurface aeration devices. This infusion of devices coupled with the equally numerous masstransfer models used for this evaluation has produced a highly confusing situation as regards measured performance.

The appearance of new exotic subsurface aeration systems accentuates the importance of a common analytical procedure. While the relative performance of any given system will correlate rather strongly to the mass-transfer model used for its evaluation, the model used does not necessarily provide an accurate representation of the system mass-transfer capabilities for comparative purposes. In many instances, the manner of analysis is completely neglected when the efficiencies of several devices are compared.

The primary intent of this paper is to present a rigorously complete analytical procedure for evaluating subsurface aeration systems. Examination of the surface aeration analytical technique and its underlying assumptions constitutes the initial phase of this treatment. Comprehending the surface aeration model and its implications is critical to evolving a phenomenologically correct subsurface model.

## SURFACE AERATION

Although no industry "standard" currently exists, the most commonly accepted method for evaluating the performance of aeration equipment is non-steady-state reaeration of water. This test procedure, along with the chemical correction for the Winkler titration analysis, has been well documented in the literature. 1—4 The data obtained by this

procedure establish a consistent basis to compare surface aeration performance.

Two additional methods that have been used for evaluating aeration performance are steady-state sodium sulfite oxidation and biological oxygen uptake. Each presents inherent test problems. 5 The sulfite oxidation technique, which involves simultaneous diffusion and chemical reaction, can result in a significantly different overall mass-transfer rate than that associated with just a physical gas absorption process. The theory of this combined effect is well established. 6,7 Tests on actual waste systems are highly dependent on biological parameters, which in themselves are difficult to evaluate and verify. Presently, there is no satisfactory method for accurately measuring oxygen transfer capabilities under biological process conditions. Hence, the effectiveness of aeration systems is not readily comparable with these procedures, and nonsteady-state reaeration of clean water is the preferred test method.

For surface aeration, a first-order, masstransfer model is used to characterize the oxygen-uptake rate and obtain the overall oxygen mass-transfer coefficient from the concentration-time history. The rate of oxygen transfer described by this clean water model is given as

$$\frac{W}{10^6} \frac{dC}{dt} = K_L a(T) (C^* - C)$$
 (1)

where

C\* = Dissolved oxygen (bo) saturation concentration (mg/l) for pure water at test conditions of temperature (T) and barometric pressure,

C = Bulk-average DO concentration (mg/l) in the basin water at time t,

 $K_L a(T) = \text{Overall liquid-phase oxygen mass-transfer coefficient at test conditions } [kg/mg/l \cdot h (lb/hr/ppm)],$ 

t = Time (hour), and

W = Weight of water in the aeration basin, [kg (lb)].

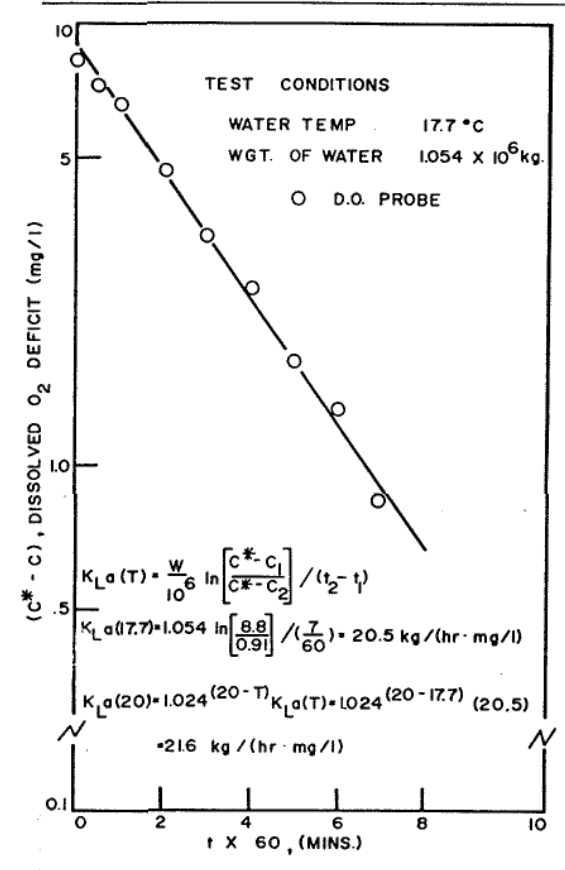


FIGURE 1. Mass-transfer coefficient determination—surface model.

There are several implicit assumptions related to this model

- Mass transfer occurs at the surface where the oxygen concentration and partial pressure of the gas phase remain constant.
- Equilibrium prevails at the gas-liquid interface and is expressed by Henry's Law.
- The liquid film constitutes the major resistance to mass transfer. Thus, the overall oxygen mass-transfer coefficient,  $K_L a(T)$ , depends only on water temperature and the partial pressure of oxygen in the gas phase (that is barometric pressure and oxygen concentration in gas).
- Effects of air temperature, wind velocity, and relative humidity (the prevailing environmental conditions other than pressure) are not significant.
- A "well mixed" condition exists in the basin and a significant bulk DO value can be particularized from sample point measurements.

Integration of Equation 1 yields an expression for the concentration profile as a function of time

$$C = C^* - (C^* - C_o) \times \exp \left\{ -\frac{10^6}{W} K_{La}(T) (t - t_o) \right\}$$
 (2)

where

 $C_o$  = Initial DO concentration (mg/l) at time  $t_o$ .

This result is the characteristic transient response of a first-order system to a step-forcing function, which in this instance is the constant surface saturation concentration,  $C^*$ . The first-order solution has particular significance pertaining to subsurface aeration analysis as noted in subsequent discussion. The logarithmic form of this expression

$$K_L a(T) = -\frac{W}{10^6} \ln \left[ (C^* - C)/(C^* - C_o) \right] / (t - t_o)$$
 (3)

is more familiar as it permits the value of the overall oxygen mass-transfer coefficient to be determined directly from the data as illustrated in Figure 1.

Effect of temperature on  $K_L a(T)$  is delineated by

$$K_L a(20) = K_L a(T) \theta^{(20-T)}$$
 (4)

in which

 $K_L a(20) = \text{Overall}$  liquid-phase oxygen mass-transfer coefficient at 20°C [kg/mg/l·h] and  $\theta = \text{Temperature correction factor.}$ 

Although there is some disagreement regarding the value of  $\theta$ , the most widely accepted value is 1.024 (literature values reported range from 1.012 to 1.047). <sup>8,9</sup>

This brief re-examination of the surface aeration model emphasizes the importance of recognizing that specific assumptions are necessary to obtain a closed form solution such as Equation 2. Before applying this model to a particular process, the validity of these fundamental assumptions should first be established. Additionally, the review of this model constitutes the basis for developing the subsurface aeration model.

### SUBSURFACE AERATION

With the preceding discussion as foundation, it is now possible to explore the submerged aeration system. The subsurface aeration

process can be defined as a two-phase (liquidgas) contacting process in which oxygen transfer from the gas to liquid phase occurs when the gas phase is continuously released below the free surface. Through the combined effects of turbulence, buoyancy, and interfacial tension, 10 the gas phase is fragmented as it is released and assumes a size distribution of rising bubbles. Exchange of the oxygen from the gas to liquid occurs during the processes of bubble formation, release, and ascension. This rate of oxygen transfer is dependent on the relative rate of ascent, bubble size, partial pressure of oxygen, temperature, and driving force (the difference between the liquid-film oxygen concentration in equilibrium with the gas bubble and the bulk-liquid DO content). Additionally, the oxygen transfer is influenced by the dispersion and coalescence characteristics produced through turbulent recirculation patterns existing in the basin.

In an unsaturated liquid, the volume of a gas bubble rising toward the free surface can vary through the concerted effects of two opposing influences. Because of the concentration difference between the bulk fluid and liquid film surrounding the bubble, there is a continued exchange from the bubble to the liquid and this dissolution process produces a decrease in mass of the bubble. At the same time, however, the decrease in hydrostatic pressure experienced with the bubble ascension affects expansion. It is clear that the bubble, which forms the elementary mass-transfer unit in the subsurface system, encounters a complex and variable equilibrium condition with respect to its position, rate of oxygen exchange, and rate of rise in the liquid-phase environment. (That is, the bubble surface area, concentration, pressure, and liquid concentration all change simultaneously.) The model as defined for surface aeration is clearly neither applicable to subsurface operations nor are results obtained from its use with this type of system significant.

To develop a relevant and tractable analysis technique requires not only restrictive assumptions, but also a mathematical scheme that retains some semblance of consistency with the phenomena. Thus, the approach chosen for the subsurface aeration process analysis is the concept of a semiflow-batch reactor system that considers mass transfer across the gasliquid interfaces in the absence of chemical reaction. In the semiflow-batch operation, one fluid (the gas phase in this case) is continuously passed through a vessel that contains a uniform distribution of a second fluid

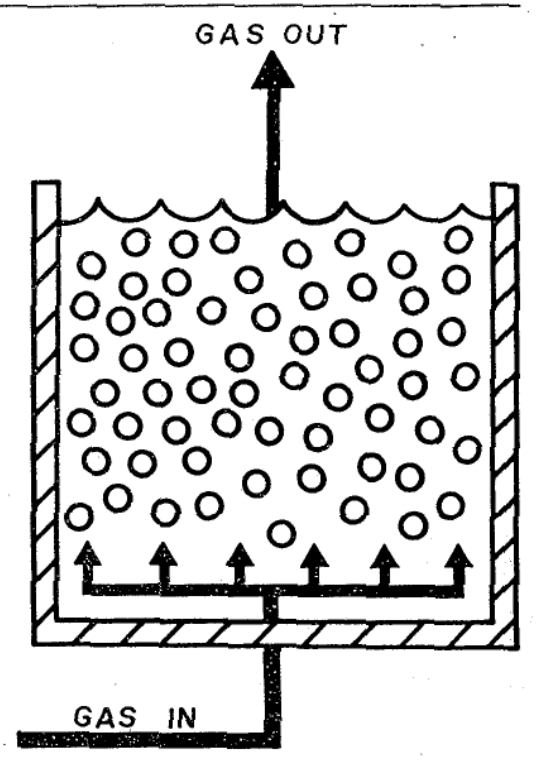


FIGURE 2. Plug-flow gas—well-mixed liquid semiflow-batch system.

(liquid phase). The liquid is retained within the reactor and is assumed "well-mixed." (The DO concentration of the liquid phase is time-dependent but spatially invariant during the test.) Figure 2 illustrates this situation. The oxygen content in the gaseous phase is dependent on both bubble residence time and vertical position.

Other assumptions imposed on this system are

- Only the transfer of a single gas component, oxygen, is considered. (The transfer of nitrogen, carbon dioxide, and other gases is neglected).
- The process is conducted under isothermal conditions. (Both the gas and liquid phases are assumed to be at the same temperature throughout the test.)
  - The liquid-film resistance is controlling.
- The overall oxygen mass-transfer coefficient is considered constant during a test and is dependent only on the liquid temperature. (The mass-transfer coefficient is independent of time and position of bubbles in the tank.)
- The equilibrium relationship is described by Henry's Law.

• The gas flow rate for a given test is constant and is described by a uniform distribution of rising bubbles across the tank crosssection.

With the semiflow reactor configuration and the above suppositions, a model for the isothermal behavior of a submerged aeration system can be derived. Briefly, examining the oxygen mass-balance equation for the gas phase produces an expression for the oxygen mole fraction as a function of vertical position and liquid no concentration. This profile is then integrated over the vertical distance to define the average oxygen mole fraction value for the driving force of the liquid-phase model. (It is presumed that in the liquid-phase equation the mass-transfer rate can be characterized by an average driving force similar to that of the surface model). This substitution leads to the determination of the overall oxygen mass-transfer coefficient.

The differential equation of continuity for the oxygen component in a rising gas bubble is given as

$$\frac{\partial}{\partial t} \left( \frac{P V_B}{RT} y \right) + v_b \frac{\partial}{\partial Z} \left( \frac{P V_B}{RT} y \right) \\
= -K_G a' P V_B \left( y - \frac{CH}{P} \right) \quad (5)$$

where

a' =Ratio of bubble surface area to bubble volume  $(m^{-1})$ .

C = Dissolved oxygen molar concentration in liquid phase (g/mole/l),

 $H = \text{Henry's constant } (kN \cdot m/g/mole),$ 

 $K_G = \text{Overall gas-phase oxygen mass-transfer coefficient } (g/\text{mole/kN} \cdot h),$ 

 $P = Pressure (kN/m^2),$ 

R = Universal gas constant (kN·m/g-mole·°K),

T = Absolute temperature (°K),

t = Time (hour),

 $v_b = \text{Bubble rise velocity (m/sec)},$ 

 $V_B = \text{Bubble volume (m}^3),$ 

y = Oxygen mole fraction in gas phase, and

Z = Vertical distance through liquid phase (m).

(Script notation is used to denote quantities expressed in molar units as opposed to similar quantities expressed in non-molar units).

Inasmuch as the oxygen content of the gas phase instantaneously present in the tank is small compared with the total quantity of oxygen passed through the tank during a reaeration test, the local time rate of change in gas-phase mass transfer is negligible. That

is, the changes that occur during the bubble residence time are insignificant when compared with changes that take place in the vertical direction. Hence, the time derivative term in Equation 5 is neglected and only convective mass transfer is considered. Neglecting this term does not make Equation 5 time independent, however, because C is a function of time.

Although the overall gas-phase oxygen masstransfer coefficient is used in Equation 5, the assumption of a liquid-film controlled process and the usual combined resistance approach defines  $K_G$  as

$$K_G = K_L/H \tag{6}$$

wher

 $K_L = \text{Overall liquid-phase oxygen mass-transfer coefficient (m/h)}.$ 

Additionally, in Equation 5, the bubble parameters, a',  $v_b$ , and  $V_B$  and the pressure, P, are dependent on the vertical position, Z, of the bubble. Substitution of the appropriate functional relationships for these parameters transforms Equation 5 into a highly nonlinear first-order differential equation in y, whose solution is intractable. However, by defining the average bubble volume

$$\langle V_B \rangle = \frac{1}{Z_s} \int_0^{Z_s} V_B dZ \tag{7}$$

where

 $Z_t$  = Vertical distance from the gas inlet to the liquid-free surface (m) and

 $\langle \rangle$  = Denotes quantity averaged over Z

this difficulty is removed as both the interfacial bubble area, a', and bubble rise velocity,  $v_b$ , are now dependent only on this quantity and can themselves be represented by average values. Equation 5 is now re-expressed as

$$\frac{dy}{dZ} + \left(\Omega + \frac{d \ln P}{dZ}\right) y = \Omega \frac{CH}{P}$$
 (8)

where

$$\Omega = \frac{K_L \langle a' \rangle RT}{H \langle v_b \rangle}.$$

Noting that at the sparge inlet,  $Z = Z_s$ , the mole fraction of oxygen is known,  $y = y_I$ , the solution to Equation 8 is

$$y = \frac{CH}{P} + \left(y_I - \frac{CH}{P_s}\right) \frac{P_s}{P} \exp{\{\Omega(Z_s - Z)\}}$$
 (9)

where  $P_s$  represents the pressure at the sparge inlet  $(P_s = P^o + \rho g Z_s, P^o)$  is the existing barometric pressure).

Using the above profile for y, the average mole fraction is determined in a similar fashion to that expressed for bubble volume. Thus, substituting Equation 9 into

$$\langle y \rangle = \frac{1}{Z_s} \int_0^{Z_s} y dZ \tag{10}$$

vields

$$\langle y \rangle = \frac{\ln (P_s/P^o)}{(P_s - P^o)} \left\{ CH + (P_s y_I - CH) \right.$$

$$\left. \times \left[ 1 - \frac{\Omega}{\rho g} \frac{(P_s - P^o)}{\ln (P_s/P^o)} \right] \exp(\Omega P_s/\rho g) \right\} \quad (11)$$

after neglecting the higher order terms obtained from the integration. With a representative average oxygen mole fraction in the gas phase established, the oxygen mass balance in the liquid phase is characterized by

$$V_L \frac{dC}{dt} = K_L \langle a' \rangle n \langle V_B \rangle V_L (C_d^* - C) \quad (12)$$

 $C_d^*$  = Dynamic molar po saturation concentration  $(C_d^* = P_d^*\langle y \rangle / H)$ 

n = Number of bubbles per unit volume of liquid (m-3),

 $V_L$  = Volume of liquid phase (m<sup>3</sup>), and  $P_d^*$  = Dynamic equilibrium pressure associated with  $\langle y \rangle$  and  $C_d^*$  by Henry's

Letting the mass-transfer area per unit volume of liquid phase be designated as

$$a = n\langle a' \rangle \langle V_B \rangle \tag{13}$$

Equation 12 takes the form

$$\frac{dC}{dt} = K_L a(P_d *\langle y \rangle / H - C) \qquad (14)$$

The expression is a first-order differential equation closely paralleling the surface model (Equation 1), and whose solution resembles the form of Equation 2. The primary differences in these relationships are that the overall oxygen mass-transfer coefficient,  $K_L a$ , is no longer expressed in an explicit fashion and the form of Pa\*, the dynamic equilibrium pressure, is as yet undefined.

Because both the average mole fraction and liquid-phase oxygen balance, (Equations 11 and 14) are valid throughout the unsteadystate reaeration test, it is useful to evaluate these relationships as the uptake time becomes In these circumstances, the net oxygen mass-transfer rate approaches zero and the measured dynamic saturation concentration,  $C_d^{\infty}$ , has been reached. This saturation value is a function of many parameters and, therefore, should be measured for each test condition. Because no oxygen is transferred from the gas stream at  $t = \infty$ , the average mole fraction equals y<sub>I</sub>. These conditions vield

$$P_d^{\infty} = \frac{C_d^{\infty} H}{y_I} \tag{15}$$

from Equation 14, and rearranging Equation 11 for C<sup>∞</sup> provides

$$C_{d}^{\infty} = \frac{y_{I}}{H} \frac{\left[\frac{(P_{s} - P^{o})}{\ln{(P_{s}/P^{o})}} - \zeta' P_{s}\right]}{(1 - \zeta')}$$
(16)

$$\zeta' = \left[1 - \frac{\Omega}{\rho g} \frac{(P_s - P^o)}{\ln (P_s/P^o)}\right] \exp(\Omega P_s/\rho g)$$

is considered the characteristic dynamic subsurface aeration (DSA) number. The results of the last two expressions clearly demonstrate that the dynamic equilibrium pressure at time infinity is not a simple quantity but is dependent on variable operating conditions related to the bubble mechanics of the system under investigation.

The measured dynamic saturation concentration, Cdo, may be rewritten in a more familiar form

$$C_d^{\infty} = \left[ \frac{C_{BOT} - C_{TOP}}{\ln (P_s/P^o)} - \zeta' C_{BOT} \right] /$$

$$(1 - \zeta') \quad (17)$$

where

$$C_{BOT} = y_I P_s / H$$
 and  $C_{TOP} = y_I P^o / H$ ,

which represent the liquid concentration at the gas inlet and free surface, respectively.

There are several interesting observations apparent from Equation 17. The first is if the value of the DSA number, I', is zero, the relationship reduces to the form of the logarithmic mean saturation concentration because the logarithm of the pressures is equal to the logarithm of the concentrations. The use of a logarithmic mean saturation value at any time other than that corresponding to saturation (for  $\zeta' = 0$ ) is erroneous. Second, depending on specific operating conditions, the value of ζ' will be nonzero and, hence, the bulk saturation concentration will deviate from a true logarithmic mean saturation value. Third, by expanding the terms in Equation 16, it may be demonstrated that the expression for  $C_d^{\infty}$  reduces to surface saturation as the sparge

depth approaches the surface.

Although the variable nature of  $\langle y \rangle$  and  $P_d^*$ requires the direct measurement of the dynamic saturation concentration in the basin, the form of Equation 17 provides a basis for interpreting its operation dependence. Specifically, once operating criteria for a specific test are established, the value of the DSA number \( \cap{'} \) is determined and remains constant for the entire test. Hence, the only variable quantities are the first two terms, which as a function of time during the test are dependent on the offgas concentration (y). In allowing them to vary as a function of the average mole fraction of oxygen in the system at any time and using this condition in Equation 17 provides not only the variable attributes of the changing equilibrium required, but also the mechanism for defining a variable average dynamic saturation concentration as a function of time. In using this result, a method for determining the overall oxygen mass-transfer coefficient is established and this procedure is discussed in the following section.

### APPLICATION OF MODEL

One of the important conclusions established in the analysis of the previous section was that the integration of the liquid phase equation, Equation 14, produced a first-order solution. Returning to nonmolar notation, the solution takes the form

$$C = C_d^{\infty} - \exp(K_1 + K_2 t) \tag{18}$$

where  $K_1$  and  $K_2$  are arbitrary constants that incorporate the overall mass-transfer coefficient in an implicit fashion, not easily segregated.

The first-order nature of the concentration profile is of consequence because it represents the embarkation point in the evaluation procedure for the subsurface aeration system. Once the concentration-time uptake data are recorded it is used to obtain the parameters of Equation 18. For the curve fitting or parameter estimation problem, the objective is to obtain parameters that provide predictive values in close agreement with the experimental data. The quantity used most often to gauge this agreement is termed the residual sum of squares (R.S.S.) and is defined as

R.S.S. = 
$$\sum_{i} \frac{1}{\sigma_{i}^{2}} (C_{OBS,i} - C_{CALC,i})^{2}$$
 (19)

in which  $C_{OBS,i}$  represents the experimental

average concentration,  $C_{\text{CALC},i}$  the calculated average concentration value predicted by the model, and  $\sigma_i^2$  the variance related to experimental error all corresponding to time  $t_i$ . Once a model is specified, the best parameters are determined by minimizing the quantity R.S.S.

The experimental form of Equation 18 is clearly nonlinear in nature with respect to the pertinent parameters to be determined. Depending on the initial specification of the problem, two different parameter estimation problems exist. These are briefly summarized as follows:

Problem	Specify	Calculate
1	$C_i$ , $t_i$	$K_1, K_2, C_d^{\infty}$
2	$C_i, t_i, C_d^{\infty}$	$K_1, K_2$

The error structure of the data should also be determined in conjunction with the curve fit process because  $\sigma_i^2$  represents a weighting factor that reflects the relative precision of the data. Although there are certain risks in using the value of  $C_d^\infty$  observed directly from allowing the test to proceed to a "saturation" point, it is nevertheless more appropriate and the method of choice. An excellent detailed review of the intricacies encountered in the curve fitting procedure is provided by Boyle et al. 11

Once the predictive concentration profile is defined (Figure 3), it is possible to differentiate the curve at the respective sample times,  $t_i$ , to provide the corresponding oxygen-transfer rates,  $OR_i$ , because

$$OR_i = \frac{W}{10^6} \frac{dc}{dt} \bigg|_{t_i} \tag{20}$$

At this point, it is necessary to digress briefly to develop the relationship between the oxygentransfer rate and the average oxygen mole fraction in the off-gas exiting the basin, (y). From the assumption of no nitrogen transfer taking place, the average mole fraction of oxygen is expressed as

$$\langle y \rangle = \frac{Y}{Y+J} \tag{21}$$

where

Y = Weight ratio of oxygen to nitrogen, kgO<sub>2</sub>/kgN<sub>2</sub> and

J = Molecular weight ratio of oxygen to nitrogen equal to 1.143 O<sub>2</sub>/kg N<sub>2</sub>.

For a constant gas flow rate, the nitrogen flow rate is obtained from the air flow rate at the sparge inlet, thus

$$G = 0.0555Q$$
 ( $G = 1.574$  scfm) (22)

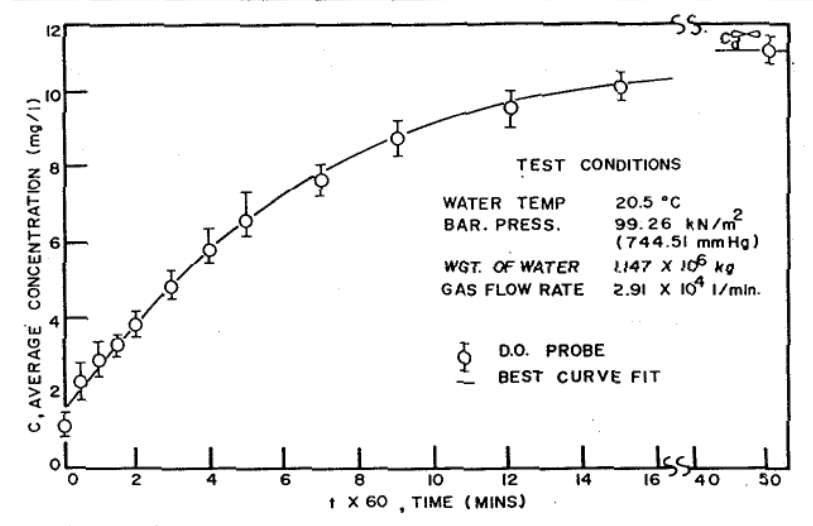


FIGURE 3. Submerged reaeration concentration—time history.

where

G = Nitrogen flow rate, kg/h and

Q = Air flow rate, 1/min.

Remembering that the time derivative in the gas-phase continuity equation was insignificant, the use of an average oxygen mole fraction allows the gas phase to be considered "well-mixed" (Figure 4), and the overall oxygen mass balance at any time  $l_i$  is now rewritten as

$$G(Y_I - Y_i) = OR_i \tag{23}$$

where

 $Y_I$  = Sparge inlet weight ratio of oxygen to nitrogen at any time (0.302 kg/kg) and

 $Y_i$  = Weight ratio of oxygen to nitrogen at time  $t_i$  (kg/kg).

Rearranging Equation 23 for Vi yields

$$Y_i = Y_I - OR_i/G \tag{24}$$

This expression allows calculation of the oxygen mole fraction  $\langle y_i \rangle$  of the off-gas and correspondingly the dynamic saturation concentration at any time,  $t_i$ . The values of  $C_{BOT}$  and  $C_{TOP}$  are now defined as

$$C_{TOP} = C_{HB}^*(T)(y_I/0.21)$$
  
 $C_{BOT} = C_{HB}^*(T)(y_I/0.21)(P_s/P^o)$  (25)

where

 $C_{HB}^*(T) = \text{Handbook po saturation concentration for pure water at test conditions and 21% oxygen.}$ 

From Equation 17, a time-dependent average

saturation concentration is now defined for use in the liquid-phase mass balance equation

$$C_d^*(t_i) = \left[ \frac{(C_{BOT} - C_{TOP})}{\ln (P_t/P^o)} \frac{\langle y_i \rangle}{y_I} - \zeta C_{BOT} \right] /$$

$$(1 - \zeta) \quad (26)$$

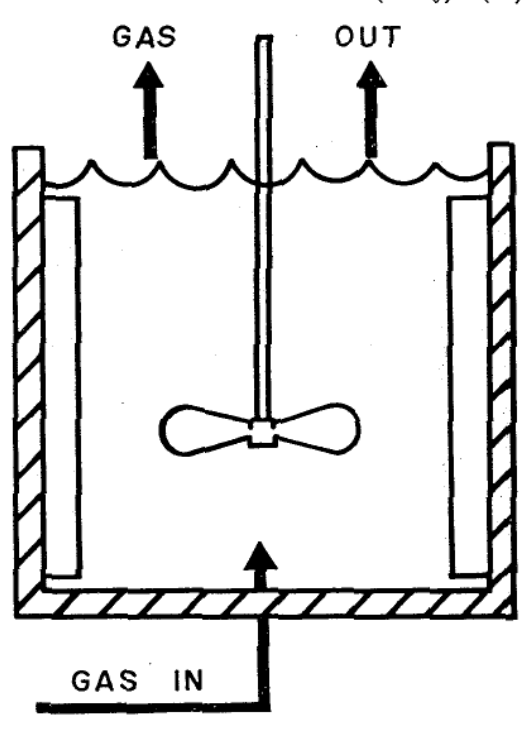


FIGURE 4. Well-mixed gas--well-mixed liquid semiflow-batch system.

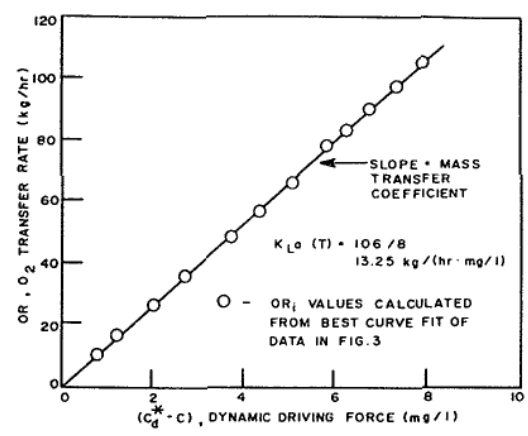


FIGURE 5. Mass-transfer coefficient determination—submerged model.

The value of the DSA number,  $\zeta$ , is determined by calculation using the saturation concentration obtained by direct measurement and the condition  $C_d^*(t=\infty)=C_d^\infty$ . Thus, rearranging Equation 26 with this condition, the DSA number is computed for the data in Figure 3 as

$$\zeta = \left[ C_d^{\infty} - \frac{(C_{BOT} - C_{TOP})}{\ln (P_{BOT}/P_{TOP})} \right] / (C_d^{\infty} - C_{BOT}) 
= \left[ 11.21 - \frac{(13.75 - 8.915)}{\ln (153.1/99.26)} \right] / 
= -0.0207.$$
(11.21 - 13.75)

Knowing the oxygen-transfer rates, average liquid concentration and average saturation concentration for each sample time produces an over-specified system of simultaneous equations of the form

$$OR_{1} = K_{L}a(T)[C_{d}^{*}(t_{1}) - C_{1}]$$

$$OR_{2} = K_{L}a(T)[C_{d}^{*}(t_{2}) - C_{2}]$$

$$OR_{i} = K_{L}a(T)[C_{d}^{*}(t_{i}) - C_{i}]$$

or in matrix notation

$$OR = K_L a(T) \lceil C_d^*(t) - C \rceil \tag{27}$$

If the data from Figure 3 are analyzed in the above fashion, a linear plot of oxygen-transfer rate, OR, versus dynamic dissolved oxygen deficit,  $[C_d^* - C]$  is obtained and is shown in Figure 5.

The solution for the overall oxygen masstransfer coefficient is then accomplished by matrix inversion such that

$$K_L a(T) = OR[C_d^*(t) - C]^{-1}$$
 (28)

(This represents the slope of the line in Figure 5.) The oxygen-transfer rate and weight ratio at zero DO content is then determined from the simultaneous solution of

$$Y_o = Y_I - OR_o/G \quad \text{and} \quad (29)$$

$$OR_o = K_L a(T) C_d^*(t_o)$$
 (30)

where the zero subscript refers to conditions at zero DO content. This amounts to a trialand-error solution technique. With this solution, the absorption efficiency of the unit is then defined by

$$E = 1 - Y_o/Y_I \tag{31}$$

For the example presented, the calculated values of the above quantities determined in this manner are respectively

$$K_L a(T) = 13.25 \text{ kg/mg/l} \cdot \text{h},$$
  
 $OR_o = 118.8 \text{ kg/h},$   
 $Y_o = 0.228 \text{ kgO}_2/\text{kgN}_2, \text{ and}$   
 $E \times 100 = 24.3\% \text{ O}_2 \text{ absorbed}.$ 

The calculated value of  $OR_o$  is now checked against the value obtained from the slope at zero do of the best curve fit of the data as an unbiased estimate of the mass-transfer rate. A nonlinear least-squares analysis of the data shown in Figure 3 yields the concentration profile

$$C = 11.21 - \exp(2.295 - 9.244t).$$

Using Equation 20 with this profile yields an oxygen-transfer rate of 118.9 kg/h, which is in very close agreement with the  $OR_o$  value calculated using the procedure outlined.

This solution at test conditions is then translated to standard conditions in the following manner. Using the temperature correction equation, Equation 4, the overall oxygen mass-transfer coefficient is corrected to 20°C.

$$K_L a(20) = 1.024^{(20-T)} K_L a(T).$$

The standard oxygen-transfer rate and weight ratio are again computed from simultaneous solution of the counterparts to Equation 29 and 30

$$Y_o(20) = Y_I - SOR/G$$
 and (33)

$$SOR = K_L a(20) C_d * 20(t_o)$$
 (34)

where  $C_d^*_{20}(l_o)$  now refers to standard conditions. This value is obtained as follows. The measured dynamic saturation value,  $C_d^*$ 

$$(t = \infty)$$
, is corrected to 20°C by

$$C_{d}^{*}_{20}(t = \infty) = 9.17(y_{I}/0.21)$$
  
  $\times [C_{d}^{*}(t = \infty)/C_{HB}^{*}(T)]$  (35)

Values of  $C_{BOT20}$  and  $C_{TOP20}$  are determined from

$$C_{BOT20} = C_{HB}^*(20)(y_I/0.21)(P_s'/P^{o'})$$
 (36)

and

$$C_{TOP20} = C_{HB}^*(20)(y_I/0.21)$$
 (37)

where

$$P_s' = P^{o'} + \rho g Z_s$$
 and  $P^{o'}$  is standard pressure (101.33kN/m<sup>2</sup>).

Using the dynamic saturation value at 20°C,  $C_d*_{20}(t=\infty)$ , a new value of the DSA number,  $f_{20}$ , is generated (as previously demonstrated for f) and the value of  $C_d*_{20}(to)$  is then established as

$$C_{d}^{*}_{20}(\text{to}) = \left[ \frac{C_{BOT20} - C_{TOP20}}{\ln (P_{s}'/P^{o'})} \frac{\langle y_{o} \rangle}{y_{I}} - \zeta_{20}C_{BOT20} \right] / (1 - \zeta_{20})$$
(38)

Correspondingly, the standard absorption efficiency is then

$$E(20) \approx 1 - Y_o(20)/Y_I.$$
 (39)

Performing these computations for the example yields the following values at standard condition:

$$K_L a(20) = 13.10 \text{ kg/mg/l·h},$$
  
 $SOR = 119.7 \text{ kg/h},$   
 $Y_o(20) = 0.228 \text{ kgO}_2/\text{kgN}_2, \text{ and}$   
 $E(20) \times 100 = 24.5\% \text{ O}_2 \text{ absorbed}.$ 

## CONCLUSIONS

Reaeration of water for subsurface aeration was examined to develop an appropriate model for evaluating submerged aeration process equipment on a standard basis. A unified semiflow-reactor approach was presented and shown consistent with the phenomena of subsurface aeration.

The results indicate that the method of evaluation presented is superior to the other techniques for several reasons

- The value of DO used for saturation is the directly observed one, which in general does not agree with the value obtained by calculation in other procedures.
  - The oxygen-transfer rate arrived at from

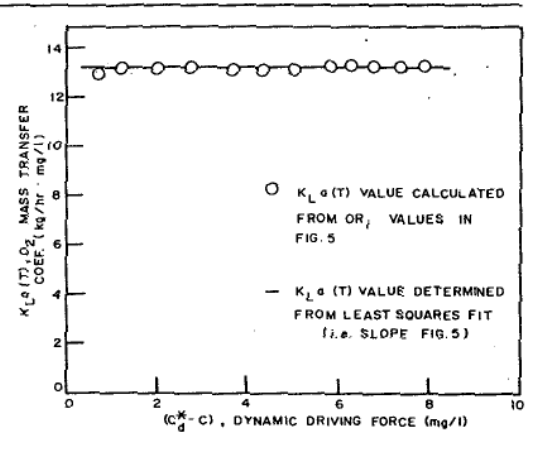


FIGURE 6. Constancy of mass-transfer coefficient versus dynamic driving force.

the model consistently provides a value in rather close agreement with that obtained from the slope of the best curve fit of the data as an independent check. Larger deviations in the rate are observed with other analytical techniques.

- Examination of data with this analytical method demonstrates that while the point oxygen-transfer rates and driving forces over the run vary by a factor of 3 or 4 or greater (example presented is a factor of 9.5), the overall oxygen mass-transfer coefficient remains relatively constant (Figure 6). This provides verification of one of the major assumptions made in the development of the model.
- The model recognizes that there are distinct differences in the type of aeration device used and provides the means to characterize these differences in an experimental fashion, \$\zeta\$, the dynamic subsurface aeration number.
- The approach provides a standardized basis for separating the mass-transfer evaluation from performance for various types of submerged aeration devices—long lacking in this field.

It is hoped that others involved in the aeration industry will move to adopt a standardized procedure and viewpoint in this form that will permit extension of the concepts presented herein for a more complete understanding of the process fundamentals.

#### ACKNOWLEDGMENTS

Credits. The work described in this paper is part of the research effort at Mixing Equipment Company, a Unit of General Signal, in the field of subsurface aeration. The aeration

test work was performed by the members of the firm's research and development department. David Grinnell developed the creative programming necessary for rapid analysis of test data.

This paper was presented at the 50th Annual Conference of the Water Pollution Control Federation, Philadelphia, Penn., October 2-7, 1977.

Authors. Michael B. Lakin and Ronald N. Salzman are respectively, Senior Research Engineer and Director of Research and Development, Mixing Equipment Co., Inc., a Unit of General Signal Corp., Rochester, N.Y.

## REFERENCES

- Landberg, G. G., "Methods and Procedures for Testing Surface Aerators." Presented at Amer. Soc. Mech. Engr.—Amer. Inst. Chem. Engr. Joint Conference on Stream Pollution and Abatement, New Brunswick, N. J. (June 1969).
- Landberg, G. G., et al., "Experimental Problems Associated with the Testing of Surface Aeration Equipment." Water Res., 3, 445 (1969).
- Kalinske, A. A., et al., "Cobalt Interference in the Non-Steady State Clean Water Test." Water & Sew. Works, 120, 54 (1973).

- Lakin, M. B., "Chemical Catalyst Interference in the Winkler Titration Determination of Dissolved Oxygen—A Method for Correction." Water Res., 10, 961 (1976).
- McWhirter, J. R., "Fundamental Aspects of Surface Aerators and Design." Proc. 20th Industrial Waste Conference, Purdue Univ. West Lafayette, Ind., 75 (1965).
- Astarita, G., "Mass Transfer and Chemical Reaction." Elsevier, Amsterdam, Netherlands (1967).
- Levenspiel, O., "Chemical Reaction Engineering." 2nd Ed., John Wiley and Sons, Inc., New York, N. Y. (1972).
- Eckenfelder, W. W., Jr., and O'Connor, D. J., "Biological Waste Treatment." Pergamon Press Ltd., Oxford, Great Britain (1961).
- Lakin, M. B., "Temperature Effects on Oxygen Mass Transfer Coefficient." Unpublished Research Report, Mixing Equipment Co., Rochester, N. Y. (1975).
- Levich, V. G., "Physiochemical Hydrodynamics." Prentice-Hall, Inc., Englewood Cliffs, N. J. (1962).
- Boyle, W. C., et al., "Pitfalls in Parameter Estimation for Oxygen Transfer Data." Proc. 28th Industrial Waste Conference, Purdue Univ., West Lafayette, Ind., 645, (1973).